Journal of Proteomics 177 (2018) 21–30

Contents lists available at ScienceDirect

Journal of Proteomics

journal homepage: www.elsevier.com/locate/jprot

Forensic proteomics for the evaluation of the post-mortem decay in bones

Noemi Procopio[a], Anna Williams[b], Andrew T. Chamberlain[c], Michael Buckley[a,*]

[a] Manchester Institute of Biotechnology, The University of Manchester, 131 Princess Street, Manchester, M1 7DN, UK
[b] School of Applied Sciences, University of Huddersfield, Queensgate, Huddersfield, HD1 3DH, UK
[c] School of Earth and Environmental Sciences, The University of Manchester, Stopford Building, 99 Oxford Road, Manchester, M13 9PG, UK

ARTICLE INFO

Keywords:
Bone proteomics
Forensic proteomics
Post-mortem interval
Biglycan deamidation

ABSTRACT

Current methods for evaluation the of post-mortem interval (PMI) of skeletal remains suffer from poor accuracy due to the great number of variables that affect the diagenetic process and to the lack of specific guidelines to address this issue. During decomposition, proteins can undergo cumulative decay over the time, resulting in a decrease in the range and abundance of proteins present (i.e., the proteome) in different tissues as well as in an increase of post-translational modifications occurring in these proteins. In this study, we investigate the applicability of bone proteomic analyses to simulated forensic contexts, looking for specific biomarkers that may help the estimation of PMI, as well as evaluate a previously discovered marker for the estimation of biological age. We noticed a reduction of particular plasma and muscle proteins with increasing PMIs, as well as an increased deamidation of biglycan, a protein with a role in modulating bone growth and mineralization. We also corroborated our previous results regarding the use of fetuin-A as a potential biomarker for the estimation of age-at-death, demonstrating the applicability and the great potential that proteomics may have towards forensic sciences.

Significance: The estimation of the post-mortem interval has a key role in forensic investigations, however nowadays it still suffers from poor reliability, especially when body tissues are heavily decomposed. Here we propose for the first time the application of bone proteomics to the estimation of the time elapsed since death and found several new potential biomarkers to address this, demonstrating the applicability of proteomic analyses to forensic sciences.

1. Introduction

Post-mortem interval (PMI) estimation is one of the most debated themes in forensic sciences, with new studies published regularly but remaining weaknesses in relation to their accuracy and applicability [1,2]. Although some attempts have been made to develop a universal PMI estimation formula applicable to decomposing corpses exposed to the surface as well as to buried bodies [3], this was shown to be affected by regional variables that render it ineffective on a global scale [4]. The complexity of this estimation is due to the fact that after death, bodies experience a complicated set of physical, biological and chemical changes that are subjected to great variability depending on exogenous and endogenous factors including body size, age, pathologies, traumas as well as typical environmental parameters (temperature, humidity, soil composition, etc.), burial depth (if buried) or other burial conditions (such as deposition of the body in air or indoors), accessibility of the carcass to insects and/or scavengers, among many others [5]. Furthermore, the estimation of the PMI may be even more challenging in cases of bodies found in water [6]. With reference to these scenarios, one proposed method to address this issue is the macroscopic and microscopic evaluation of the presence of adipocere in the recovered body. However, this also exhibited some weaknesses, especially when the levels of adipocere were evaluated within the bone structure of bodies with prolonged PMIs [7]. This large number of variables makes the estimation of the PMI a controversial topic, with increasing timescales further reducing its accuracy [8]. Despite the substantial number of investigations aimed at estimating the PMI of a carcass during the first stages of decomposition [8–13], the task becomes much more difficult in more advanced stages of decomposition, particularly when only skeletal remains survive.

The canonical method for the determination of the PMI from bones is based on a visual and external assessment of the progression of taphonomic processes that affect bones, and in particular on the evaluation of the extent of “subaerial bone weathering” that induces cracking and delamination of bones exposed to the open air in a time-dependent way [14]. However, rates of bone weathering are affected by

* Corresponding author.
E-mail address: m.buckley@manchester.ac.uk (M. Buckley).

https://doi.org/10.1016/j.jprot.2018.01.016
Received 22 December 2017; Received in revised form 25 January 2018; Accepted 29 January 2018
Available online 31 January 2018

the presence of vegetation and by environmental conditions at the locality of deposition (humidity, temperature, etc.) [14], and the evaluation of this parameter is only applicable when bones are exposed on the ground surface. Alternative methods for estimating the PMI include the study of entomological succession to evaluate the time elapsed since death [15], but severe limitations (e.g. no specific insect activity during the dry stage of decomposition [16], weakness of the method when the body is buried in the soil at different depths [15], etc.) leave demand for the development of new techniques to better address this question. Another parameter that can be used is the colour change of bones during the decomposition process, but this may be strongly influenced by several factors including the soil type in which bones were buried and by its mineral composition and the organic matter within it, as well as by the presence of adipocere and/or lipids [17] or the effects of haemolysis [17,18].

More recently, molecular taphonomic approaches have been proposed for the estimation of PMI, for example by assessing the levels of DNA preservation in bones associated with prolonged PMIs [19,20]. However, it has been found that environmental factors (e.g. humidity [19], depth of burial or soil geochemistry [20]) significantly affect the quality of DNA recovered, leaving the field open to new strategies to approach this question. It is also known that microscopic alterations of bone samples may reflect the time elapsed from death, where several recent studies have focused on the application of different visualization methods to investigate the PMI of bone remains, such as infrared (IR) microscopic imaging [21–23], micro-computed tomography analyses coupled with energy dispersive X-ray mapping [23] and fluorescence spectroscopy [24], or a combination of these with traditional approaches [25]. However, the applicability of these methodologies to forensic cases remains limited (e.g. ability to discriminate between forensic and archaeological specimens, but incapacity to accurately estimate PMIs on the order of magnitude of weeks or months), with further studies required. Other approaches have been explored to address this issue, such as the evaluation of the microbial community associated with decaying bones to differentiate between phases of skeletal decay [26,27]. However, the applicability of this method is confined to the distinction between partially skeletonized/completely skeletonized and dry remains [26] or to limited PMIs (48 days as the maximum interval) [27].

1.1. Bone composition and protein diagenesis

Bones are composed essentially of an inorganic matrix (hydroxyapatite crystals (HA), ~50–70%), an organic phase constituted mostly by proteins (~90% collagenous proteins and ~10% non-collagenous proteins and proteoglycans) and by lipids, and water [28–30]. Some non-collagenous proteins (NCPs) and proteoglycans (PGs) can strongly bind the HA matrix (e.g. osteocalcin, bone sialoprotein, osteopontin, fibronectin, decorin, biglycan and fibromodulin) due to the amphoteric nature of the HA that promotes the binding of acidic and basic proteins [31]. This interaction protects proteins from degradation and prevents their disruption after the organism's death [30,31]; for this reason, they are also found frequently in archaeological specimens [30,32,33]. Other proteins frequently found in bone samples, including archaeological remains, are abundant plasma proteins such as albumin [34,35], prothrombin [33,36], haemoglobin [37] and coagulation factors [33].

Despite the great longevity of these biomolecules in bone [38,39], the complexity of the bone proteome decreases with geological time due to the leaching of minerals and proteins to the burial environment [40,41], the latter related to the hydrolysis of peptide bonds that are thermodynamically unstable and that makes proteins to be more fragmented and damaged [42]. In particular, bone collagen hydrolyses over time, and after ~10,000–30,000 years only a little intact collagen remains (except for specimens deposited in cold and/or dry environments) [42]. Some other NCPs are thought to be more resistant to hydrolysis than collagen, and they may be successfully recovered even when only little intact collagen is still present [43]. Wadsworth and Buckley [39] used shotgun proteomics to demonstrate how the complexity of the bone proteome can become reduced in ancient bones, focusing attention on NCPs and exploring the role that the thermal history has on the degradation of these biomolecules [39]. In addition to protein hydrolysis, cumulative protein damage through deamidation is also observed [44]; in particular, this non-enzymatic post-translational modification (PTM) occurs naturally in asparagine (Asn) and glutamine (Gln) residues, which are converted respectively into aspartic acid (Asp) and glutamic acid (Glu) both *in vivo* [45,46] and post-mortem [47–49]. Promisingly there appears to be some correlation between the glutamine deamidation ratios of peptides from several different proteins in archaeological specimens and their geological age [50].

However, in contrast to our knowledge of protein decay over long periods of archaeological and geological time, little is known about the protein degradation in buried bones in shorter, forensic timescales. Although we have previously utilised proteomic analyses to look for specific biomarkers for age-at-death (AAD) estimation in a simulated forensic scenario [51], there are no studies linking the proteomic profiling of forensic bones with known PMIs. Therefore, the aims of the work presented here were to evaluate the applicability of proteomic analyses to simulated forensic burials with different PMIs in order to explore bone diagenesis from a proteomic perspective and to seek specific biomarkers that may be useful for PMI estimation of skeletal remains.

2. Material and methods

Experimental burials were conducted at the HuddersFIELD outdoor taphonomy facility (University of Huddersfield, UK), situated on grassy farmland in West Yorkshire (UK) with a soil pH ~7.2. The experiment was conducted following the guidelines of the U.K. Department for Environment, Food and Rural Affairs (DEFRA). Daily temperatures and rainfall measurements were obtained from the local Weather Station (Watson W-8681) which is situated ~5 km northwest of the burial site. The weather station collects data every 30 s and updates the website www.weatherforce.org.uk, in which daily records from 2010 to the present day are available to the public (Supplementary Figs. S1 and S2).

Four juvenile pig (*Sus scrofa*) carcasses (mean weight = 8.1 kg, approximate age at death = three to five weeks) were obtained as a commonly used analogue for humans in decomposition studies [52,53]. The pigs, which had died naturally from unknown causes, were frozen within 48 h of death and defrosted 24 h before the start of the experimental burials. We consider the PMI as set to zero on the day in which all of the carcasses were buried under ~40 cm soil, located ~90 cm away from each other to reduce the likelihood of cross-contamination. The pigs were protected by steel gabion cages that were buried inside the graves to limit the action of scavengers; each cage was also wrapped in fly netting to limit the activity of small rodents or birds on the buried bodies, while still allowing access by arthropods. Data loggers (Tinytag Plus 2, Gemini Data Loggers) with probes were used to constantly measure the temperature of the soil in contact with each of the four carcasses. Lysimeters, each under 75 psi pressure, were also placed inside the cage in contact with the soil in which the pigs were buried to allow the regular extraction of leachate from the soil surrounding the pigs. The graves were completely infilled with soil, in order to mask the burial site and to better simulate a forensic scenario. To reduce the potential damage due to the activity of scavengers, each grave was covered with a wooden palette that allowed the rainfall water to reach the soil but that prevented the area to be accessed by scavengers or by unauthorized personnel.

The four carcasses were left in the soil for different time intervals (see Table 1); after the selected time interval, the bodies were partially excavated to collect one of the two tibiae, keeping the disturbance of

Table 1
Specimens used in the study and information about the samples extracted for the experiment.

Pig ID number	Skin colour	Weight (kg)	Approximate age (weeks)	Sex	PMI after first tibia recovery	PMI after second tibia recovery
1	White band ("saddle"), black fur	4.5	3–4	Male	1 month	1 year
2	White	6.1	3–4	Male	2 months	1 year
3	White	10.8	4–5	Male	4 months	1 year
4	White, black dots on the back	11.0	4–5	Male	6 months	1 year

the rest of the carcass to a minimum in order to avoid displacing of the other skeletal elements.

During this phase, soil samples above the carcass were collected for further analyses. All the samples (bones and soil) were frozen within a few hours after their collection and kept at −20 °C until they were analysed. After the samples were extracted, the bodies were re-covered with the grave infill, and left to continue to decompose until they reached one year PMI. After one year, all four carcasses were collected on the same day as well as samples of the soil that had been in direct contact with the remains. All animal material was removed from the site after retrieving the tibiae for subsequent analysis. Tibiae were collected in separate bags, frozen and further processed.

Dentist's Protaper Universal Hand Files used for the drilling were purchased from Henry Schein Minerva Dental (UK). Acetonitrile (ACN) was purchased from Fisher Scientific, and formic acid (FA) was purchased from Fluka (UK) (via Sigma-Aldrich, UK). Tris, dithiothreitol (DTT), iodoacetamide (IAM), trifluoroacetic acid (TFA), guanidine hydrochloride (GuHCl), ammonium acetate (AMAC) and phosphate-buffered saline (PBS) were purchased from Sigma- Aldrich (UK), and 10 kDa molecular weight cut-off (MWCO) ultrafilters were acquired from Vivaspin (UK). Sequencing grade trypsin was purchased from Promega (UK), and OMIX C18 reversed-phase Zip-Tips were acquired from Agilent Technologies.

Two batches of samples were processed at different times. The first batch, which included the four tibiae collected after one, two, four and six months PMI, was processed as soon as the last tibia was collected (i.e. after six months from the start of the experiment). The second batch included the four tibiae collected after one year PMI, which were processed at the end of the experiment. Bones were defrosted in a fume cupboard and left in a solution of water and 20% PBS for one hour at room temperature to remove soil residues from the samples. The surface of each bone was then gently scraped to remove any further soil and vegetation, and following Procopio and Buckley [51] the midshaft of the tibia was sampled in quintuplicate using sterile dentist's hand files. Approximately 25 mg of bone powder was collected five times per bone, then each sample was demineralized for six hours at 4 °C with 10% FA and the insoluble fraction incubated with GuHCl for 18 h at 4 °C. The buffer was then exchanged into 50 mM AMAC with 10 kDa MWCO filters and then the samples were reduced with 5 mM DTT for 40 min at room temperature, alkylated with 15 mM IAM for 45 min in the dark at room temperature and quenched with a further amount of 5 mM DTT. Proteins were then digested with 1 μg of trypsin at 37 °C for five hours. Digestion was stopped by adding 1% TFA (making 0.1% TFA), and then samples were desalted, purified and concentrated with OMIX C18 reversed-phase Zip-Tips following manufacturer's protocols. Peptides were eluted from the Zip-Tips in 100 μL of 50% ACN/0.1% TFA, then samples were dried under the fume cupboard for one day and then they were resuspended in 20 μL of 5% ACN/0.1% TFA for subsequent LC-MS/MS analysis.

Resuspended samples were analysed by LC-MS/MS using an UltiMate 3000 Rapid Separation LC (RSLC, Dionex Corporation, Sunnyvale, CA, USA) coupled to an Orbitrap Elite (Thermo Fisher Scientific, Waltham, MA, USA) mass spectrometer (120 k resolution, full scan, positive mode, normal mass range 350–1500). Peptides were separated on an Ethylene Bridged Hybrid (BEH) C18 analytical column (75 mm × 250 μm i.d., 1.7 μM; Waters) using a gradient from 92% A (0.1% FA in water) and 8% B (0.1% FA in ACN) to 33% B in 44 min at a flow rate of 300 nL min − 1. Peptides were then automatically selected for fragmentation by data-dependent analysis; six MS/MS scans (Velos ion trap, product ion scans, rapid scan rate, centroid data; scan event: 500 count minimum signal threshold, top 6) were acquired per cycle, dynamic exclusion was employed, and one repeat scan (i.e., two MS/MS scans total) was acquired in a 30 s repeat duration with that precursor being excluded for the subsequent 30 s (activation: collision-induced dissociation (CID), 2+ default charge state, 2 m/z isolation width, 35 eV normalized collision energy, 0.25 activation Q, 10.0 ms activation time).

Peptide mass spectra were then searched against the Swiss-Prot database for matches to primary protein sequences using the Mascot search engine (version 2.2.0.6; Matrix Science, London, UK), without specific taxonomy filters. Each search included the fixed carbamidomethyl modification of cysteine (+57.02 Da) and the variable modifications for deamidation (asparagine to glutamine, +0.98 Da) and oxidation of lysine, proline, and methionine residues (all +15.99 Da) to account for post-translational modifications and diagenetic alterations; the oxidation of lysine and proline is equivalent to hydroxylation. Enzyme specificity was trypsin with up to two missed cleavages allowed; mass tolerances were set at 5 ppm for the precursor ions and 0.5 Da for the fragment ions. All spectra were considered as having either 2+ or 3+ precursors.

Progenesis software (version 2.0; Nonlinear Dynamics, Newcastle, UK) was used for identification and the obtainment of relative quantitation of the proteins present in each sample; the software can quantify the ionic abundance of unique peptides, and then data are normalized to allow specific comparisons. In this way, both within-sample comparisons and between different replicates or experimental conditions comparisons can be achieved, and biological differences can be highlighted and identified. Ions with a score < 41 were excluded from the analysis in order to ensure that only ions with amino acid sequences possessing sufficient homology to known sequences were retained, according to Mascot evaluation of the peptide score distribution. Furthermore, proteins with only one or less unique peptides were excluded from the study to increase the reliability of the results. Peptides identified were expected to be matched with "*Sus scrofa*" proteins but given the lack of an appropriate database thoroughly inclusive of this taxon (e.g., lacking complete COL1A1 and COL1A2 sequences), those that were not matched as expected (Supplementary Table S1) were searched with BLAST against "*Sus scrofa*" and were considered to be "pig proteins" if a 100% match was achieved (Supplementary Table S2). While for the first batch all the samples (five replicates for each bone) gave a good alignment score, the second batch (Supplementary Tables S3 and S4) was affected by some technical issues encountered during the LC-MS/MS analyses, and this resulted in fewer samples available for data analysis (four replicates were available for pig 1 and 3, and five replicates were available for pig 2; pig 4 was not included in the analysis because only one sample was available). STRING software (version 10.5) was used to represent protein-protein interactions, where the line thickness indicates the strength of data support with a minimum required interaction score of 0.4 (medium confidence).

PCA was calculated on normalized abundances exported from Progenesis using R software with the package FactoMineR, and plots were produced using the Python programming language (Python

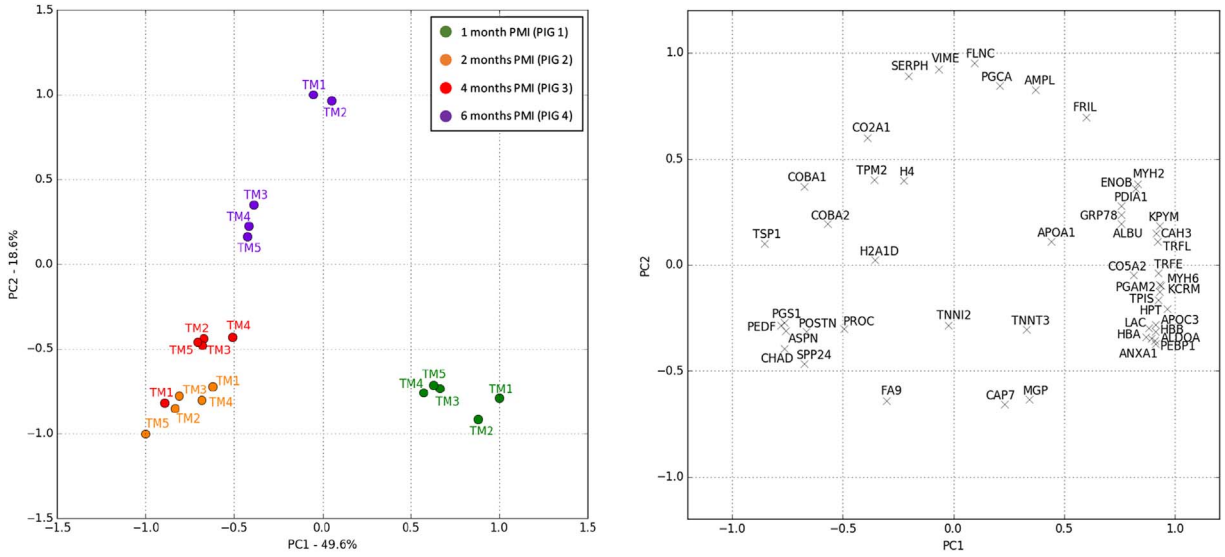

Fig. 1. PCA biplot (left) with quantitative proteomic data on the midshaft of the tibia (TM) from four piglets buried and recovered after increasing PMIs (different colours indicate different animals; five replicate subsamples were collected for each of the areas tested and are numbered 1–5 on the biplots) and a variables factor map (right) of the PCA for the first two components.

Software Foundation, https://www.python.org/) using only proteins whose ANOVA p values were smaller than 0.01, to exclude proteins whose levels were similar between different samples and were not contributing to the separation of different samples.

3. Results

3.1. Proteome abundance and complexity - with increasing PMIs

The first batch of samples (tibia samples collected after one, two, four and six months PMI) resulted in the acquisition of 34,865 spectra. After data refinement we matched 66 different *Sus scrofa* proteins of which 48 gave an ANOVA p value < 0.01 when their relative abundances were evaluated, indicating statistical difference between different PMIs (Fig. 1, left). The five replicates collected from each pig clustered together showing a good biological reproducibility between tibia samples collected from the midshaft and confirming what was previously observed by Procopio et al. [51]. The tibia collected from one month PMI clustered away from tibiae collected after two and four months in the 1st principal component, themselves clustering similar to each other in the 1st but distinct in the 2nd principal component. The tibia collected after six months gave greater change in the 2nd principal component, suggesting that substantial changes in the observed proteomes take place between one and two months PMI (1st component), and then minor changes happen between two, four, and six months PMI (2nd component). As shown by the vector map (Fig. 1, right), the majority of proteins (28 out of 48) were more abundant in the tibia collected after one month PMI compared with the others, as expected. However, there were also other proteins that appeared to be more abundant in samples collected after two, four and six months (proteins on the left-had side of the vector map).

However, the aim of the paper was to focus on the proteomic variability directly linked with differences in the PMIs, and for this reason we focused our analyses on the 28 proteins which were statistically more abundant in samples collected after one month PMI than in the others. After the refinements already specified in the Methods section, proteins belonging to the 75th percentile were reported in a bar chart (Fig. 2). It appears that the main changes were completed by four months PMI, with little evidence for significant change between four and six months.

The protein interaction pathway between the above-mentioned list of proteins showed a significant enrichment in the number of interactions (p value = 2.8e-11), with enrichments in some biological processes (11 proteins involved in small molecule metabolic process, p value = 0.0007 and eight involved in wound healing, p value = 0.0004), in molecular functions (14 proteins involved in ion binding, p value = 0.01) and in some cellular components (13 proteins present in the extracellular exosome, p value = 2e-6, and 8 in the cytoplasmic membrane-bounded vesicle lumen p value = 2e-12). When the KMEANS clustering algorithm was then applied to cluster proteins in the network (k = 3), we obtained a major cluster with most of the proteins in the network (light blue; Fig. 3), a smaller cluster (red; Fig. 3) including beta-enolase, triosephosphate isomerase, protein disulfide-isomerase and collagen alpha-1(V) chain (here named ENO3, TPI1, P4HB and COL5A1), and a final one including two muscle proteins (myosins 2 and 6, named MYH2 and MYH6) and lactotransferrin (here named LTF), the last one being not linked with the other two (green cluster; Fig. 3).

These proteins were then manually divided into four groups characterized by different trends. The first group (A) contained proteins where abundance was considerably reduced from one month to six months PMI, the second (B) where abundances decreased strongly between two and four months PMI, the third (C) where they decreased in a less pronounced way throughout the experiment, and the fourth (D) included two proteins where abundances decreased rapidly after the first two months and then remained constant after increasing PMIs (Fig. 4).

Proteins in group A are, in particular, the two subunits of the haemoglobin protein (alpha and beta, HBA and HBB) that are involved in the transport of oxygen, and three more proteins including serotransferrin (TRFE), a plasma protein which transports iron, lactotransferrin (TRFL), a protein similar to serum transferrin with a function in bone turnover, and triosephosphate isomerase (TPIS), a protein involved in the gluconeogenesis pathway. In group B, there are two types of myosin (MYH2 and MYH6) which are the most abundant muscle proteins, two other muscle proteins (beta-enolase (ENOB) and creatine kinase M-type (KCRM)) and one other plasma protein (haptoglobin (HPT)) that binds free plasma haemoglobin and that also has an antibacterial activity. In group C, we found three plasma proteins (albumin (ALBU), apolipoproteins A-1 and C-3), collagen type 5 (CO5A2), matrix Gla protein (MGP) that inhibits bone formation, and finally protein disulfide-isomerase (PDIA), with a catalytic activity for

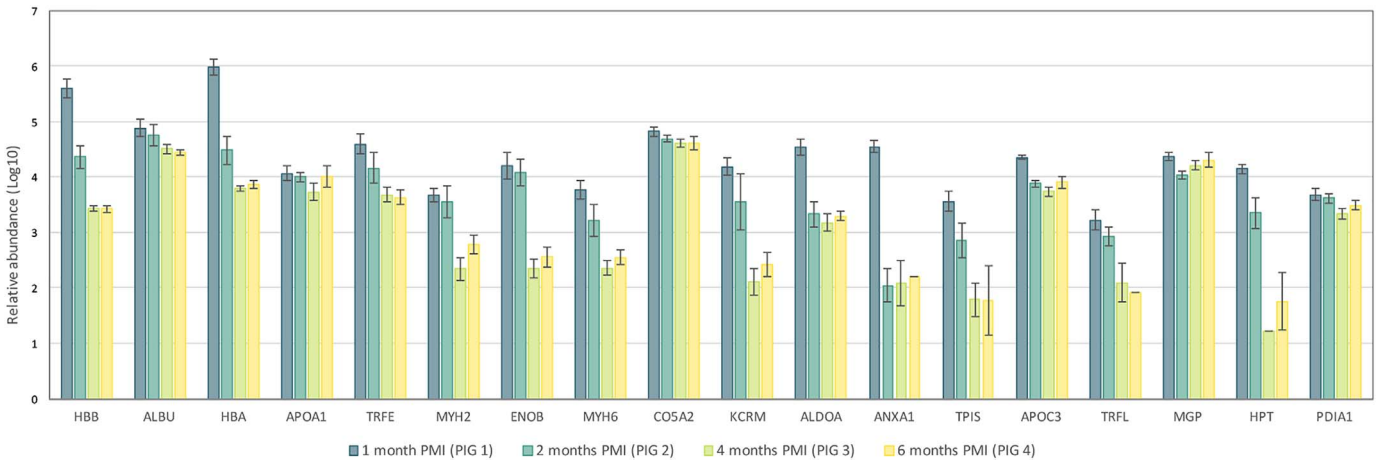

Fig. 2. Bar chart of the proteins most abundant in samples collected from pig 1 after one month PMI and belonging to the 75th percentile (sorted by confidence score, ANOVA p value < 0.01). Their relative abundance is reported in a Log10 scale, and the value represents the average obtained between five samples collected on the same bone.

the rearrangement of disulphide bonds in proteins. In the last group, there is fructose-bisphosphate aldolase A (ALDOA), which plays a role in glycolysis and gluconeogenesis, and annexin A1 (ANXA1), which has a role in the innate immune response.

The relative abundance of fetuin-A, a serum protein whose abundance in bones has been shown to be negatively correlated with the biological age of the animals [51], was also evaluated in this study, to verify if there were any differences between the different animals that were estimated to have a similar biological age (between 3 and 5 weeks). As expected, we did not find any statistical significance in the variability of fetuin-A abundances across different bone samples (ANOVA p value = 0.13), showing that different animals with the same

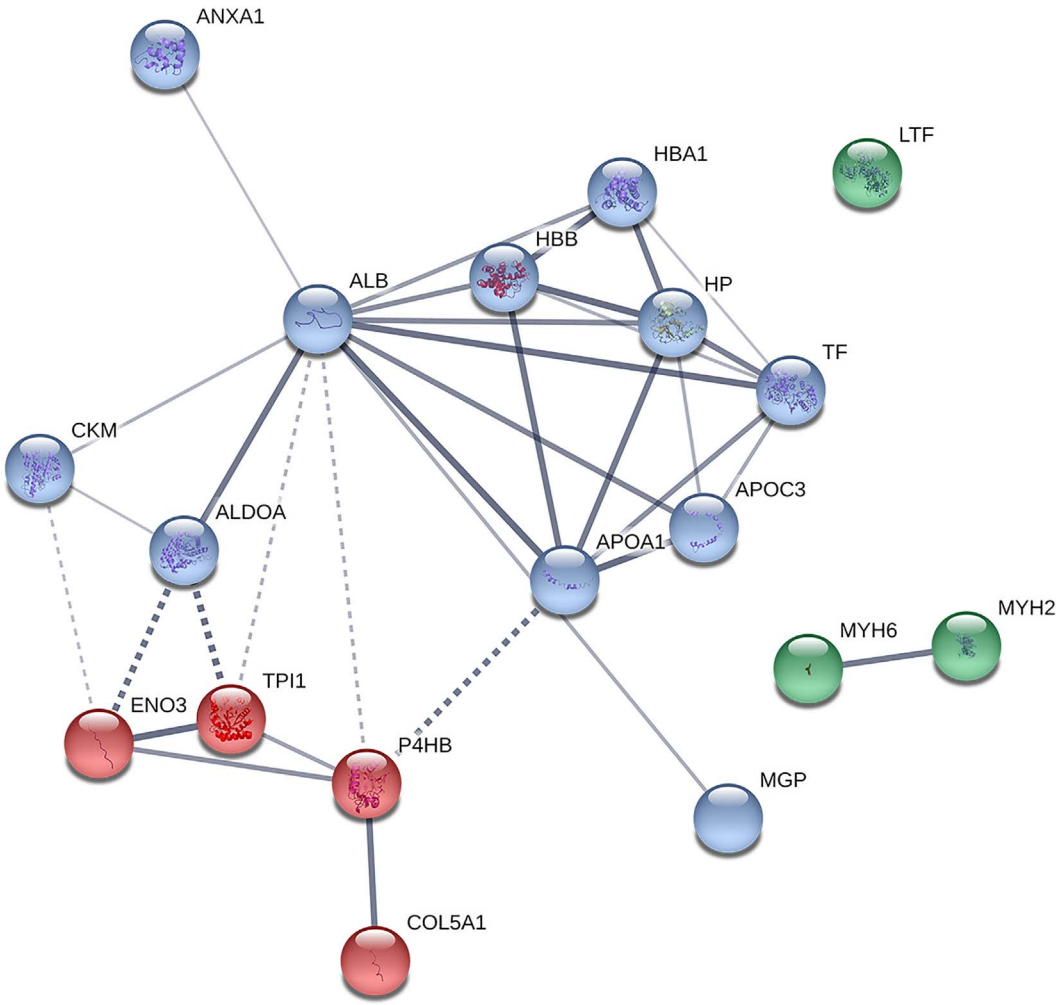

Fig. 3. STRING interaction pathway of the proteins most abundant in samples collected from pig 1 after one month PMI and belonging to the 75th percentile (sorted by confidence score, ANOVA p value < 0.01).

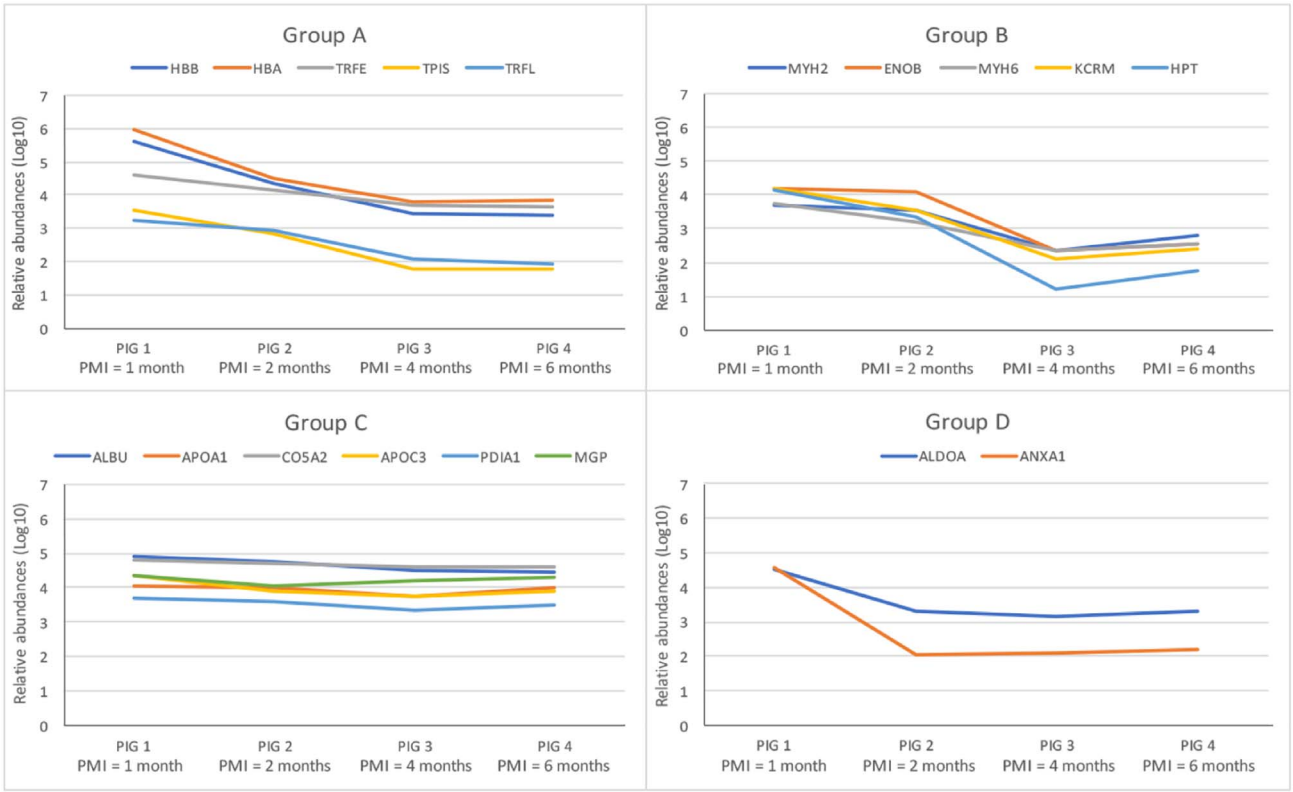

Fig. 4. Different trends observed for specific groups (A–D) of proteins after increasing PMIs. The y axis indicates the Log10 of the relative abundance of the proteins recovered from bones after different PMIs.

biological age may have similar contents of fetuin-A in bones, despite their different PMIs.

After one year PMI, the tibiae from three of the skeletons that remained buried (e.g. bones from the limb that were not collected during the first exhumation) were collected and the proteomes were analysed to compare the proteome recovery after short and prolonged PMIs. Even though we have shown previously that LC-MS/MS analyses performed on different days may result in poor reproducibility of the relative abundances calculated in each run [51], we compared the previous batch of analyses with this one to verify the presence/absence of specific proteins after one year PMI. From this second batch of analysis we matched only 19 proteins that satisfied the above-mentioned threshold criteria (29% of the proteins compared with the previous batch of analyses). In particular, they were six types of collagen (CO1A1, CO1A2, CO5A1, CO5A2, COBA1 and COCA1), six serum proteins (albumin, C-reactive protein, coagulation factor IX, fetuin-A, prothrombin and vitamin-K dependent protein C), four small-leucine rich proteoglycans (SLRPs) (biglycan, decorin, asporin and lumican), one small integrin-binding ligand, N-linked glycoprotein (SIBLINGs) (bone sialoprotein), the glycoprotein SPARC and the calcium-binding protein nucleobindin-1. Between them, nine proteins did not show statistical differences between the various groups (e.g. different animals from which bones were collected), and the other ten on the contrary showed inter-animal variability (ANOVA score < 0.05, Supplementary Table S5). Interestingly, the serum protein fetuin-A is among the proteins which did not show any statistical variability between different specimens, showing a lack of significant variability among different individuals.

3.2. Proteome deamidations with increasing PMIs

Among the list of proteins obtained during the first batch of analyses, we selected the proteins that matched against the "*Sus scrofa*" species after the Mascot searches, and for each we looked for particular peptides present both in their "non-deamidated" and "deamidated N/Q" forms (e.g. peptides which contained either an asparagine deamidation (N) or a glutamine deamidation (Q)). For these proteins, we calculated the ratios of the abundances of deamidated/non-deamidated peptides, and then an average ratio for each of the animals analysed.

Interestingly, we did not find glutamine deamidations that satisfied these requirements, but found five proteins characterized by peptides that were both "non-deamidated" and "N-deamidated": albumin, biglycan, fetuin-A, secreted phosphoprotein 24 and vitamin K-dependent protein C. The general trend showed decreased deamidation levels in samples from pig 1 and 2, and then increased deamidation ratios for bones recovered after longer PMIs. However, among the list of selected proteins, the only one where peptide deamidation ratios were statistically different after different PMIs was biglycan (PGS1, Fig. 5) in which a non-significant (Student's *t*-Test p value = 0.27) decrease of deamidations between one and two months PMI is followed by a robust and statistically significant (ANOVA p value = 0.0008) increase after four and six months PMI. The peptide selected for this specific analysis was "VGVNDFCPVGFGVKR", which was reported to be present in samples both in the unmodified form and with an asparagine deamidation in position "4".

4. Discussion

4.1. Changes in the bone proteome with increasing post-mortem interval

In this study, we explored the changes in the bone proteome that are associated with increasing PMIs, to make for the first time an evaluation of the effects that the decomposition of whole bodies within the burial environment may have on their proteins during a forensic timeframe. For this reason, we investigated the variability of bone proteomics data collected from pig carcasses that were buried for increasing PMIs (one, two, four, six and twelve months) in order to understand how proteins leach from the bodies and/or decay inside the tissues, as well as to look

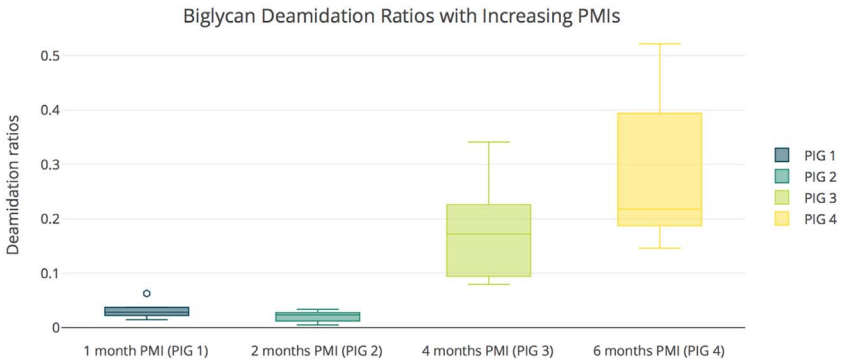

Fig. 5. Box plot representing deamidation ratios calculated for the four tibias collected after prolonged PMIs (one, two, four and six months respectively). Each box represents five replicates that have been analysed per individual.

for specific markers that may help in the estimation of the PMI.

PCA performed on the relative abundances of the proteins extracted from the four bones (Fig. 1) showed four well-separated clusters, with the first cluster (one month PMI) being separated along the 1st component from the other three clusters, and the remaining three being separated from each other mostly along the 2nd component. The 1st component accounted for the 49.6% of the overall variability, proving that the major variations that could be observed in bone proteomes take place between the first and the second month PMI, along with the decomposition of soft tissues that were mostly decomposed but still partially present after one month since death. The 2nd component accounted for 18.6% of the overall variability, suggesting that the variations observed on the PCA along this component have a minor role compared with those observed along the 1st component. In particular, we found some proteins to be relatively more abundant in samples with prolonged PMIs, such as serpin, periostin or vimentin (Fig. 1, these and other proteins abundant in tibiae from pig 2, 3 and 4 are displayed on the left-hand side of the vector map). On one hand, this could be related with inter-individual variability that may result in a different abundance of some proteins within some individuals; although this is a very interesting point that deserves to be explored in more detail, this is beyond the purpose of this study and for this reason we did not further investigated this aspect. On the other hand, we could hypothesize that the abundance of these proteins is similar within our samples, but the strong presence of other proteins within the tibia collected after one month may have masked the presence of these less abundant proteins during the LC/MS-MS analyses, resulting in an apparent minor abundance of those. This may highlight a weakness of the Progenesis software used, which may need to be further explored to better clarify this issue.

Focusing on the proteins of which their abundance decreased from one month PMI to prolonged PMIs, the greatest changes were recorded between one and four months PMI, whereas between four and six months we noticed only slight differences in the relative abundances of the extracted proteins (Fig. 2). Records of the temperatures from the burials (Supplementary Fig. S3) showed an increase from the time zero, in which we buried the carcasses, until four months later, followed by a decrease in temperature until it reached a minimum after nine months from the beginning of the experiments. These measurements were also in agreement with the air temperatures recorded from the local meteostation (Supplementary Fig. S1). On the contrary, we did not observe particular links between the precipitation levels and the decay of the bodies because they had substantially different trends each month (Supplementary Fig. S2). We believe that the slowdown observed for protein decay was undoubtedly linked with the environmental conditions, and in particular with the decrease of the temperatures that made the decomposition proceed slower during the winter months.

The majority of the proteins for which abundance decreased over prolonged PMIs are known to interact together, despite some being serum proteins (e.g. albumin, haemoglobin), some muscle proteins (e.g. creatine kinase M-type) and some proteins known to be involved in glycolysis and gluconeogenesis pathways (e.g. fructose-bisphosphate aldolase A) (Fig. 3). We were able to identify trends of decay for specific groups of proteins. Sometimes, protein abundances decreased rapidly after the first month post-mortem, continued to decrease between two and four months, and then became much more stable (trend observed for group A, Fig. 4), whereas for other proteins we observed only slight variations between one and two months PMI followed by a quick decrease of the abundances after two months and subsequent stabilization after four months PMI (trend observed for group B, Fig. 4). Interestingly, proteins belonging to the first group were mostly plasma proteins (HBB, HBA, TRFE, TRFL), which are all known to be present in the blood vessels and in the bone marrow; in particular, haemoglobin (HBA and HBB) is found in red blood cells that are produced in the bone marrow [54], transferrin is a plasma protein that binds iron and that travels to the bone marrow to deliver iron to new erythrocytes [55], and lactoferrin is a protein similar to transferrin which is contained in the secondary granules of neutrophils [56], that are also generated in the bone marrow [57]. In addition to these four proteins, triosephosphate isomerase (TPIS) also showed a similar behaviour to that previously shown for plasma proteins.

Previous studies showed the existence of correlations between increasing PMIs and decreasing concentrations of some plasma proteins, both in blood and in bones. In particular, the luminol test was applied to skeletal remains [58] to test the presence of haemoglobin in order to evaluate if the remains were of medico-legal interest (PMI ≤ 100 years) or of historical interest (PMI > 100 years). The luminol test, in fact, has a weaker reaction in the latter case due to the decay of haemoglobin in bones with increasing PMIs [58]. It is known that after decomposition of the soft tissues, the skeletal remains start to decompose and the haemoglobin starts to breakdown in a time-dependent manner [59]. Both the benzidine and the luminol tests were able to identify the presence of haemoglobin in old skeletal remains, but different tests resulted in different PMI thresholds for the identification of the haemoglobin (benzidine shows a greater sensitivity, with positive results obtained until 100–350 years post-mortem [60,61], whereas luminol gives positive results only with samples characterized by shorter PMIs (around 70 years [59])). However, we were not able to match any peptide with haemoglobin after one year post-mortem which may be due to the partial decay of the protein that makes it less amenable to being correctly identified using mass spectrometric methods, despite its detectability with such predictive tests in bones for prolonged times. Furthermore, in our study we used juvenile pig bones, which are thought to be more prone to diagenesis than those of adults [62], which may have also impacted upon our analyses.

In addition to haemoglobin studies, recently it has been also demonstrated that transferrin concentration in blood decreases in a linear manner during putrefaction of human blood from zero to eleven days

PMI [63], making the evaluation of transferrin levels one parameter that may have the potential to estimate the PMI of blood traces; however, this was only a preliminary study performed in the laboratory for a short time interval and was not conducted on whole bodies in a simulated forensic burial scenario as performed in our study. Costa et al. [63] found that transferrin decayed with a half-life of around one month at room temperature (21 °C), but our burial temperatures were clearly lower than 21 °C for the whole duration of the experiment (see Supplementary Fig. S3), and we believe that this caused the decay of the proteins, including transferrin, to proceed much more slowly. For this reason, we were still able to detect transferrin after six months PMI; its decrease over the time is in agreement with the findings of Costa et al. [63], and is probably due to its decay more than to its leaching from the blood vessels and the bone marrow into the surrounding environment.

Di Luca et al. recently performed a study on the proteomic characterization of post-mortem changes in porcine muscle after one, three and seven days, with the final aim of addressing the tenderness of the meat for the food industry [64]. They found that many metabolic enzymes increased in abundance between one and seven days post-mortem, but they also recorded a decrease over the ageing period of a few proteins, including triosephosphate isomerase [64]. This result corroborates our findings in that a decrease in the abundance of triosephosphate isomerase can be observed over time from one to six months post-mortem, with complete decay after one year since death. Some other studies also indicated that the level of this protein starts to decrease from slaughter until 24 h later in bovine muscle [65], which is in agreement with our observations for prolonged PMIs within the burial environment.

In addition to our findings for plasma proteins, we also observed a specific trend of decay for some other proteins that were included in a second grouping (Fig. 3) that were composed mostly of muscle proteins. Even though the tissue analysed here was bone, it is reasonable to assume that some muscle proteins were also co-extracted with the bone proteins due to the close proximity of muscle to bone and the incomplete skeletonization process after post-mortem intervals that were limited to six months in a relatively cold environment. These proteins were not identified after twelve months PMI, indicating the more complete decomposition of the surrounding soft tissues after that time interval. In this case, in contrast with what was seen previously, the decay and/or leaching of these proteins from the bodies started later; we noticed, a slight decrease in their abundances after one month, but a more substantial decrease between two and four months post-mortem. Previous studies already investigated the early stages of the post-mortem decay of muscles under controlled conditions and showed a degradation of the heavy chain of myosins due to post-mortem autolysis [66,67] as soon as the decomposition starts. This was in accordance with our findings, namely that myosin heavy chains (types two and six) are degraded over time in the burial environment, as well as beta-enolase, creatine kinase M-type and haptoglobin. The first of these, beta-enolase, is a metabolic enzyme highly expressed in muscle tissue and was previously found to be increased in abundance from one to seven days post-mortem but also highly fragmented, as indicated by the smaller molecular weight of its spots on the 2-D gel [64]; we observed here an increased decay over time (that reached its maximum after four months post mortem). We also noticed a similar trend for both creatine kinase M-type (which catalyzes the transfer of phosphate in muscle) and haptoglobin (which functions to bind free haemoglobin).

4.2. Fetuin-A and inter-individual variability

Previous studies [33,51] have demonstrated a negative correlation between the abundance of fetuin-A in bones and the biological age of the specimens, suggesting the potential use of this protein as a new biomarker for estimating the biological age of the skeletal remains for forensic applications. We verified the reliability of this approach by evaluating the abundances of fetuin-A in bones from pigs with similar biological ages, to investigate whether the inter-individual variability could affect the quality of the results. Interestingly, we did not find any statistical difference between the abundances of fetuin-A in the four tibiae we analysed, showing on the one hand little inter-individual variability, and on the other that different PMIs (spanning from one to six months) does not affect the recovery of this particular protein. Fetuin-A appears to remain stable over increasing times after death, at least within the experimental conditions tested here (bodies that were buried and left undisturbed with PMIs of months, up to one year). Fetuin-A is a serum protein produced by the liver, and its main role is the inhibition of the ectopical calcification of calcium phosphate through the formation of colloidal mineral-protein complexes (calciprotein particles, CPPs) [68,69]. Furthermore, it is one of the most abundant bone NCPs [70,71] that accumulates in calcified tissues due its great affinity with the apatite minerals, forming an integral part of the calcified matrix [72]. Its role in bone mineralization and metabolism has already been explored, and it has been shown that the absence of fetuin-A in bones causes problems in the growth of long bones due to a premature mineralization of the growth plate during endochondral ossification [68], with an observed greater cortical thickness and an increased bone mineral density [73]. Due to its great affinity with the mineral matrix of the bone, fetuin-A is protected from leaching from the bone tissue, and this allows its recovery also from archaeological specimens that are hundreds of years old [33]. Our results here are in agreement with what previously observed; in fact, fetuin-A was one of the proteins that we were still able to detect after one year PMI. Also in this case, we did not observe any statistical variability between different specimens, supporting again the previous findings.

Although fetuin-A levels did not change between the different specimens collected after the same PMI (one year), we noticed that nine proteins were characterized by different abundances across the different animals. Interestingly, when there was variability between individuals, pig 1 was always the one with higher abundances of these proteins compared with the rest. Some differences in the burial environment may have caused the observed variations (e.g. different exposure to wind/rain currents, slight variations in the preparation of the graves (differences in the amount of soil used to fill the holes), different amounts of rain water that percolated through the graves during the experiment, etc.). Moreover, there could have been some intrinsic differences within the different individuals that may have contributed to this variability (e.g. pig breed, differences in nutrition among the various pigs, pathological conditions we were unaware of, etc.). As we were not able to clarify which of these variables was the most likely cause of the observed variations, additional studies could be carried out under more controlled conditions (e.g. experimental decay in the laboratory with controlled environmental parameters) to further explore these factors.

4.3. Asparagine deamidation and post-mortem interval

The variations in the levels of deamidations among different specimens were explored in an attempt to identify correlations between increased PMIs and deamidation levels. Deamidations are non-enzymatic reactions that acts as molecular clocks during ageing phenomena, both *in vivo* [74] and post-mortem [75]. While glutamine deamidation has been studied mostly in archaeological samples due to the long lifespan of this process compared with the faster asparagine deamidation, the latter has on the contrary only been studied mostly in relation to its role in tissue ageing [75], but not for forensic purposes. We performed comparisons between the deamidation ratios of specific proteins among the different individuals to verify if the PMI affected the amount of recorded deamidations, on the assumption that the variability between different piglets was negligible (the animals had a similar biological age). Interestingly, we noticed generally fewer deamidations in samples obtained from the second pig (PMI = two

months), although this was not statistically supported. The only protein whose deamidation levels were statistically different as a function of PMI was biglycan (Fig. 5), a small leucine-rich proteoglycan highly abundant in the skeletal tissue with a role in modulating osteoblast differentiation and matrix mineralization [76], new bone formation and angiogenesis during fracture healing [77]. Intriguingly, in this case, deamidation ratios increased markedly between two and four months PMI, continued to increase but more slowly after four months, and reaching their apparent maximum abundances after approximately six months (the last time point in this study). Due to the positive correlation between biglycan deamidation and post-mortem interval, we believe that this may have potential as a biomarker that could help in the estimation of the PMI. Furthermore, this protein was still recovered after one year PMI during this investigation, and previous studies have demonstrated the long lifespan of this protein, which was extracted from archaeological specimens dating back to almost one million years ago [39]. For this reason, biglycan deamidations may become a useful post-mortem interval biomarker in forensic contexts over for prolonged timespans.

5. Conclusions

We report the first proteomic study conducted on experimental forensic specimens aimed at better understanding how proteins decay after death in bodies within a burial environment. The overall aim being to look for specific variations that occur with increasing PMIs in order to identify new potential biomarkers that may help in the evaluation of the PMI from a molecular perspective, especially when only skeletal remains are available for the analysis.

We noticed that most of the proteome changes in bones have occurred within the first four months post-mortem, and that afterwards proteins decayed in a slower way, leading to the observations of a reduced proteome complexity. Some plasma proteins, including haemoglobin A and B, transferrin and lactoferrin, and a metabolic protein (triosephosphate isomerase), decayed at a quick rate between one and four months PMI, whereas some other muscle proteins (myosin type 2 and 6, beta-enolase, creatine kinase M-type and haptoglobin) decayed slowly between one and two months PMI, but then rapidly between two and four months.

Moreover, we were also able to find a statistically significant correlation between the increase of asparagine deamidations in biglycan and the increase of PMI; we believe that this may also become a new biomarker that may help in the identification of specific PMIs ranging from one to six months.

Recently we showed that fetuin-A relative abundances correlate well with the biological age of an individual; in this work, fetuin-A was shown to be relatively stable after death in forensic contexts. Furthermore, we did not find differences in fetuin-A abundances among the various individuals, showing the lack of significant inter-individual variability and strengthening the power of this new biomarker for AAD estimation.

Further work is required to evaluate more in deeply how the proteomes decay (e.g. expanding the study to more time intervals, exploring the impact that the environmental conditions (such as the seasons in which are conducted the experiments) may have on it, or making comparisons between buried and non-buried corpses) in order to develop a mathematical model that may predict the PMI based on proteome decay and PTMs. However, this preliminary study demonstrates the applicability of proteomic analyses to forensic sciences, with the possibility to open new frontiers in particular on the estimation of the age-at-death and on the post-mortem interval, bypassing some of the limitations that occur when bones, or small fragments of them, are found on a crime scene.

Supplementary data to this article can be found online at https://doi.org/10.1016/j.jprot.2018.01.016.

Transparency document

The http://dx.doi.org/10.1016/j.jprot.2018.01.016 associated with this article can be found, in online version.

Acknowledgements

We acknowledge support from the Royal Society for funding both a Ph.D. studentship (N.P.) and university research fellowship (M.B.) under grants RG130453 and UF120473, respectively. We also acknowledge the technical support of The University of Manchester's Biomolecular Analysis core facility for mass spectrometry analyses.

References

[1] A.A. Vass, The use of volatile fatty acid biomarkers to estimate the post-mortem interval, Taphon. Hum. Remain. Forensic Anal. Dead Depos. Environ, John Wiley & Sons, 2017.
[2] A. Lodha, N. Ansari, T. Prajapati, M.V. Rao, S.K. Menon, Novel approach to determine post-mortem interval from ATPase activity, Aust. J. Forensic Sci. 49 (2017) 22–30.
[3] A.A. Vass, The elusive universal post-mortem interval formula, Forensic Sci. Int. 204 (2011) 34–40.
[4] D.L. Cockle, L.S. Bell, Human decomposition and the reliability of a “Universal” model for post mortem interval estimations, Forensic Sci. Int. 253 (2015) (136-e1).
[5] E.M.J. Schotsmans, M. Nicholas, S.L. Forbes, Taphonomy of human remains: forensic analysis of the dead and the depositional environment, John Wiley & Sons, 2017.
[6] P.A. Magni, C. Venn, I. Aquila, F. Pepe, P. Ricci, C. Di Nunzio, F. Ausania, I.R. Dadour, Evaluation of the floating time of a corpse found in a marine environment using the barnacle *Lepas anatifera* L.(Crustacea: Cirripedia: Pedunculata), Forensic Sci. Int. 247 (2015) e6–e10.
[7] E. Jopp-van Well, C. Augustin, B. Busse, A. Fuhrmann, M. Hahn, M. Tsokos, M. Verhoff, F. Schulz, The assessment of adipocere to estimate the post-mortem interval–a skeleton from the tidelands, Anthropol. Anz. 73 (2016) 235–247.
[8] B. Swift, The timing of death, in: G.N. Rutty (Ed.), Essentials Autops. Pract, Springer London, London, 2006, pp. 189–214, , http://dx.doi.org/10.1007/b136465.
[9] P.T. Garcia, E.F.M. Gabriel, G.S. Pessôa, J.C.S. Júnior, P.C. Mollo Filho, R.B.F. Guidugli, N.F. Höehr, M.A.Z. Arruda, W.K.T. Coltro, Paper-based microfluidic devices on the crime scene: a simple tool for rapid estimation of post-mortem interval using vitreous humour, Anal. Chim. Acta 974 (2017) 69–74.
[10] C. Crostack, S. Sehner, T. Raupach, S. Anders, Re-establishment of rigor mortis: evidence for a considerably longer post-mortem time span, Int. J. Legal Med. (2017) 1–4.
[11] C. Li, D. Ma, K. Deng, Y. Chen, P. Huang, Z. Wang, Application of MALDI-TOF MS for estimating the postmortem interval in rat muscle samples, J. Forensic Sci. 62 (2017) 1345–1350.
[12] R. Swain, A. Kumar, J. Sahoo, R. Lakshmy, S.K. Gupta, D.N. Bhardwaj, R.M. Pandey, Estimation of post-mortem interval: a comparison between cerebrospinal fluid and vitreous humour chemistry, J. Forensic Legal Med. 36 (2015) 144–148.
[13] T. Zerbini, L.F.F. da Silva, P.A.L. Baptista, E.S. Ikari, M.R. de Araujo, C.D.S. de André, J. da Motta Singer, F.M.M. da Rocha, E.A. Junior, C.A.G. Pasqualucci, Estimation of post mortem interval by tomographic images of intra-cardiac hypostasis, J. Forensic Legal Med. 38 (2016) 111–115.
[14] C.A. Junod, J.T. Pokines, Subaerial Weathering, J.T. Pokines, S.A. Symes (Eds.), Man. Forensic Taphon, CRC Press, 2013, pp. 287–314.
[15] C. Pietro Campobasso, G. Di Vella, F. Introna, Factors affecting decomposition and Diptera colonization, Forensic Sci. Int. 120 (2001) 18–27.
[16] M. Lee Goff, Early post-mortem changes and stages of decomposition in exposed cadavers, Exp. Appl. Acarol. 49 (2009) 21–36.
[17] T.L. Dupras, J.J. Schultz, Taphonomic bone staining and color changes in forensic contexts, in: J.T. Pokines, S.A. Symes (Eds.), Man. Forensic Taphon, 1st ed., CRC Press, 2013, pp. 315–340.
[18] M.A. Huculak, T.L. Rogers, Reconstructing the sequence of events surrounding body disposition based on color staining of bone, J. Forensic Sci. 54 (2009) 979–984.
[19] W.L. Perry, W.M. Bass, W.S. Riggsby, K. Sirotkin, The autodegradation of deoxyribonucleic acid (DNA) in human rib bone and its relationship to the time interval since death, J. Forensic Sci. 33 (1988) 144–153.
[20] E. Hagelberg, L.S. Bell, T. Allen, A. Boyde, S.J. Jones, J.B. Clegg, S. Hummel, T.A. Brown, R.P. Ambler, Analysis of ancient bone DNA: techniques and applications, Philos. Trans. R. Soc. Lond. Ser. B Biol. Sci. 333 (1991) 399–407.
[21] C. Woess, S.H. Unterberger, C. Roider, M. Ritsch-Marte, N. Pemberger, J. Cemper-Kiesslich, P. Hatzer-Grubwieser, W. Parson, J.D. Pallua, Assessing various infrared (IR) microscopic imaging techniques for post-mortem interval evaluation of human skeletal remains, PLoS One 12 (2017) e0174552.
[22] D. Creagh, A. Cameron, Estimating the post-mortem interval of skeletonized remains: the use of infrared spectroscopy and Raman spectro-microscopy, Radiat. Phys. Chem. 137 (2016) 225–229.
[23] S. Longato, C. Wöss, P. Hatzer-Grubwieser, C. Bauer, W. Parson, S.H. Unterberger, V. Kuhn, N. Pemberger, A.K. Pallua, W. Recheis, Post-mortem interval estimation of human skeletal remains by micro-computed tomography, mid-infrared microscopic

imaging and energy dispersive X-ray mapping, Anal. Methods 7 (2015) 2917–2927.
[24] N. Hoke, A. Grigat, G. Grupe, M. Harbeck, Reconsideration of bone postmortem interval estimation by UV-induced autofluorescence, Forensic Sci. Int. 228 (2013) (176-e1).
[25] A. Amadasi, A. Cappella, C. Cattaneo, P. Cofrancesco, L. Cucca, D. Merli, C. Milanese, A. Pinto, A. Profumo, V. Scarpulla, Determination of the post mortem interval in skeletal remains by the comparative use of different physico-chemical methods: are they reliable as an alternative to ^{14}C? Homo 68 (2017) 213–221.
[26] F.E. Damann, D.E. Williams, A.C. Layton, Potential use of bacterial community succession in decaying human bone for estimating postmortem interval, J. Forensic Sci. 60 (2015) 844–850.
[27] J.L. Metcalf, L.W. Parfrey, A. Gonzalez, C.L. Lauber, D. Knights, G. Ackermann, G.C. Humphrey, M.J. Gebert, W. Van Treuren, D. Berg-Lyons, A microbial clock provides an accurate estimate of the postmortem interval in a mouse model system, elife 2 (2013) e01104.
[28] B. Clarke, Normal bone anatomy and physiology, Clin. J. Am. Soc. Nephrol. 3 (Suppl. 3) (2008) S131–9, http://dx.doi.org/10.2215/CJN.04151206.
[29] A.L. Boskey, Bone composition: relationship to bone fragility and antiosteoporotic drug effects, Bonekey Rep. 2 (2013).
[30] Y.M. Coulson-Thomas, V.J. Coulson-Thomas, A.L. Norton, T.F. Gesteira, R.P. Cavalheiro, M.C.Z. Meneghetti, J.R. Martins, R.A. Dixon, H.B. Nader, The identification of proteoglycans and glycosaminoglycans in archaeological human bones and teeth, PLoS One 10 (2015) e0131105.
[31] S.G. Rees, D.T.H. Wassell, R.J. Waddington, G. Embery, Interaction of bone proteoglycans and proteoglycan components with hydroxyapatite, Biochim. Biophys. Acta 1568 (2001) 118–128.
[32] M. Buckley, C. Wadsworth, Proteome degradation in ancient bone: diagenesis and phylogenetic potential, Palaeogeogr. Palaeoclimatol. Palaeoecol. 416 (2014) 69–79.
[33] R. Sawafuji, E. Cappellini, T. Nagaoka, A.K. Fotakis, R.R. Jersie-Christensen, J.V. Olsen, K. Hirata, S. Ueda, Proteomic profiling of archaeological human bone, R. Soc. Open Sci. 4 (2017) 161004.
[34] C. Cattaneo, K. Gelsthorpe, P. Phillips, R.J. Sokol, Detection of blood proteins in ancient human bone using ELISA: a comparative study of the survival of IgG and albumin, Int. J. Osteoarchaeol. 2 (1992) 103–107.
[35] M. Owen, J.T. Triffitt, Extravascular albumin in bone tissue, J. Physiol. 257 (1976) 293–307.
[36] E. Karlström, M. Norgård, K. Hultenby, E. Somogyi-Ganss, R. Sugars, G. Andersson, M. Wendel, Localization and expression of prothrombin in rodent osteoclasts and long bones, Calcif. Tissue Int. 88 (2011) 179–188.
[37] P.R. Smith, M.T. Wilson, Detection of haemoglobin in human skeletal remains by ELISA, J. Archaeol. Sci. 17 (1990) 255–268.
[38] H.N. Poinar, B.A. Stankiewicz, Protein preservation and DNA retrieval from ancient tissues, Proc. Natl. Acad. Sci. 96 (1999) 8426–8431.
[39] C. Wadsworth, M. Buckley, Proteome degradation in fossils: investigating the longevity of protein survival in ancient bone, Rapid Commun. Mass Spectrom. 28 (2014) 605–615, http://dx.doi.org/10.1002/rcm.6821.
[40] G. Turner-Walker, The chemical and microbial degradation of bones and teeth, Adv. Hum. Palaeopathology 592 (2008).
[41] L.D.M. Bruce, M. Rothschild, Postmortem alteration of bone and its interpretation, Skelet. Impact Dis. Bull. 33, New Mexico Museum of Natural History and Science, 2006, pp. 19–25.
[42] J.L. Bada, Amino acid cosmogeochemistry, Philos. Trans. R. Soc. Lond. Ser. B Biol. Sci. 333 (1991) 349–358.
[43] P.M. Masters, Preferential preservation of noncollagenous protein during bone diagenesis: implications for chronometric and stable isotopic measurements, Geochim. Cosmochim. Acta 51 (1987) 3209–3214.
[44] N.L. van Doorn, J. Wilson, H. Hollund, M. Soressi, M.J. Collins, Site-specific deamidation of glutamine: a new marker of bone collagen deterioration, Rapid Commun. Mass Spectrom. 26 (2012) 2319–2327, http://dx.doi.org/10.1002/rcm.6351.
[45] N.E. Robinson, A.B. Robinson, Deamidation of human proteins, Proc. Natl. Acad. Sci. U. S. A. 98 (2001) 12409–12413, http://dx.doi.org/10.1073/pnas.221463198.
[46] N.E. Robinson, B. Robinson, Molecular clocks, Proc. Natl. Acad. Sci. U. S. A. 98 (2001) 944–949, http://dx.doi.org/10.1073/pnas.98.3.944.
[47] N. Araki, M. Moini, Age estimation of museum wool textiles from *Ovis aries* using deamidation rates utilizing matrix-assisted laser desorption/ionization time-of-flight mass spectrometry, Rapid Commun. Mass Spectrom. 25 (2011) 3396–3400, http://dx.doi.org/10.1002/rcm.5237.
[48] P.G. Hains, R.J.W. Truscott, Age-dependent deamidation of lifelong proteins in the human lens, Invest. Ophthalmol. Vis. Sci. 51 (2010) 3107–3114, http://dx.doi.org/10.1167/iovs.09-4308.
[49] G. Leo, I. Bonaduce, A. Andreotti, G. Marino, P. Pucci, M.P. Colombini, L. Birolo, Deamidation at asparagine and glutamine as a major modification upon deterioration/aging of proteinaceous binders in mural paintings, Anal. Chem. 83 (2011) 2056–2064, http://dx.doi.org/10.1021/ac1027275.
[50] N. Procopio, A.T. Chamberlain, M. Buckley, Exploring biological and geological age-related changes through variations in intra- and inter-tooth proteomes of ancient dentine, J. Proteome Res. (2018) (accepted for publication), https://doi.org/10.1021/acs.jproteome.7b00648.
[51] N. Procopio, A.T. Chamberlain, M. Buckley, Intra- and Interskeletal proteome variations in fresh and buried bones, J. Proteome Res. 16 (2017) 2016–2029.
[52] F. Yan, R. McNally, E.J. Kontanis, O.A. Sadik, Preliminary quantitative investigation of postmortem adipocere formation, J. Forensic Sci. 46 (2001) 609–614.
[53] A.S. Wilson, R.C. Janaway, A.D. Holland, H.I. Dodson, E. Baran, A.M. Pollard, D.J. Tobin, Modelling the buried human body environment in upland climes using three contrasting field sites, Forensic Sci. Int. 169 (2007) 6–18.
[54] N. Mohandas, P.G. Gallagher, Red cell membrane: past, present, and future, Blood 112 (2008) 3939–3948.
[55] C.A. Finch, H. Huebers, Perspectives in iron metabolism, N. Engl. J. Med. 306 (1982) 1520–1528.
[56] N. Esaguy, A.P. Aguas, M.T. Silva, High-resolution localization of lactoferrin in human neutrophils: labeling of secondary granules and cell heterogeneity, J. Leukoc. Biol. 46 (1989) 51–62.
[57] D. Link, Mechanisms of Neutrophil Release from the Bone Marrow, (2013).
[58] J.I. Creamer, A.M. Buck, The assaying of haemoglobin using luminol chemiluminescence and its application to the dating of human skeletal remains, Luminescence 24 (2009) 311–316.
[59] F.J. Introna, G. Di Vella, C.P. Campobasso, Determination of postmortem interval from old skeletal remains by image analysis of luminol test results, J. Forensic Sci. 44 (1999) 535–538.
[60] B. Knight, I. Lauder, Methods of dating skeletal remains, Hum. Biol. 41 (1969) 322–341.
[61] F. Facchini, D. Pettener, Chemical and physical methods in dating human skeletal remains, Am. J. Phys. Anthropol. 47 (1977) 65–70.
[62] G. Grupe, Impact of the choice of bone samples on trace element data in excavated human skeletons, J. Archaeol. Sci. 15 (1988) 123–129.
[63] I. Costa, F. Carvalho, T. Magalhães, P.G. de Pinho, R. Silvestre, R.J. Dinis-Oliveira, Promising blood-derived biomarkers for estimation of the postmortem interval, Toxicol. Res. 4 (2015) 1443–1452.
[64] A. Di Luca, G. Elia, A.M. Mullen, R.M. Hamill, Monitoring post mortem changes in porcine muscle through 2-D DIGE proteome analysis of Longissimus muscle exudate, Proteome Sci. 11 (2013) 9.
[65] X. Jia, K. Hollung, M. Therkildsen, K.I. Hildrum, E. Bendixen, Proteome analysis of early post-mortem changes in two bovine muscle types: M. longissimus dorsi and M. semitendinosis, Proteomics 6 (2006) 936–944.
[66] S. Takeichi, I. Tokunaga, K. Yoshima, M. Maeiwa, Y. Bando, E. Kominami, N. Katunuma, Mechanism of postmortem autolysis of skeletal muscle, Biochem. Med. 32 (1984) 341–348.
[67] R. Lametsch, A. Karlsson, K. Rosenvold, H.J. Andersen, P. Roepstorff, E. Bendixen, Postmortem proteome changes of porcine muscle related to tenderness, J. Agric. Food Chem. 51 (2003) 6992–6997.
[68] L. Brylka, W. Jahnen-Dechent, The role of fetuin-A in physiological and pathological mineralization, Calcif. Tissue Int. 93 (2013) 355–364.
[69] J. Seto, B. Busse, H.S. Gupta, C. Schäfer, S. Krauss, J.W.C. Dunlop, A. Masic, M. Kerschnitzki, P. Zaslansky, P. Boesecke, Accelerated growth plate mineralization and foreshortened proximal limb bones in fetuin-A knockout mice, PLoS One 7 (2012) e47338.
[70] B.A. Ashton, H.-J. Höhling, J.T. Triffitt, Plasma proteins present in human cortical bone: enrichment of the αHS-glycoprotein, Calcif. Tissue Int. 22 (1977) 27–33.
[71] J.D. Termine, Non-collagen proteins in bone, Cell Mol. Biol. Vertebr. Hard Tissues. 136 (1988) 178–202.
[72] I.R. Dickson, A.R. Poole, A. Veis, Localisation of plasma α2HS glycoprotein in mineralising human bone, Nature 256 (1975) 430–432.
[73] M. Szweras, D. Liu, E.A. Partridge, J. Pawling, B. Sukhu, C. Clokie, W. Jahnen-Dechent, H.C. Tenenbaum, C.J. Swallow, M.D. Grynpas, α2-HS glycoprotein/fetuin, a transforming growth factor-β/bone morphogenetic protein antagonist, regulates postnatal bone growth and remodeling, J. Biol. Chem. 277 (2002) 19991–19997.
[74] N.E. Robinson, A.B. Robinson, Molecular clocks, Proc. Natl. Acad. Sci. U. S. A. 98 (2001) 944–949, http://dx.doi.org/10.1073/pnas.98.3.944.
[75] N.L. Doorn, J. Wilson, H. Hollund, M. Soressi, M.J. Collins, Site-specific deamidation of glutamine: a new marker of bone collagen deterioration, Rapid Commun. Mass Spectrom. 26 (2012) 2319–2327.
[76] D. Parisuthiman, Y. Mochida, W.R. Duarte, M. Yamauchi, Biglycan modulates osteoblast differentiation and matrix mineralization, J. Bone Miner. Res. 20 (2005) 1878–1886.
[77] A.D. Berendsen, E.L. Pinnow, A. Maeda, A.C. Brown, N. McCartney-Francis, V. Kram, R.T. Owens, P.G. Robey, K. Holmbeck, L.F. de Castro, Biglycan modulates angiogenesis and bone formation during fracture healing, Matrix Biol. 35 (2014) 223–231.